

Identifying the processes controlling the distribution of H₂O₂ in surface waters along a meridional transect in the eastern Atlantic

S. Steigenberger¹ and P. L. Croot²

Received 7 November 2007; revised 17 December 2007; accepted 7 January 2008; published 13 February 2008.

[1] Hydrogen peroxide (H₂O₂) is an important oxidant for many bio-relevant trace metals and organic compounds and has potential as a tracer for mixing in near surface waters. In this study we combine H₂O₂ and bio-optical measurements with satellite data for a meridional transect from 46°N to 26°S in the eastern Atlantic in order to determine the key processes affecting its distribution. Surface H₂O₂ ranged from 21–123 nmol L⁻¹, with maximum inventories (0–200 m) of 5.5–5.9 mmol m⁻² found at 30°N and 25°S. Analyses showed a strong positive correlation of surface H₂O₂ with daily irradiances and recent precipitation, though poor correlations with CDOM suggest sunlight is the limiting reactant for H₂O₂ formation. Vertical distributions of H₂O₂ were controlled by a combination of mixing processes and phytoplankton activity. The present study highlights processes controlling global H₂O₂ distributions and points towards the development of parameterization schemes for prediction via satellite data. **Citation:** Steigenberger, S., and P. L. Croot (2008), Identifying the processes controlling the distribution of H₂O₂ in surface waters along a meridional transect in the eastern Atlantic, *Geophys. Res. Lett.*, 35, L03616, doi:10.1029/2007GL032555.

1. Introduction

[2] In marine systems H₂O₂ functions as a strong oxidant or a reductant and thus it is important for the cycling of organic compounds and trace metals like Fe [Millero and Sotolongo, 1989]. H₂O₂ is the most stable intermediate in the four-electron reduction of O₂ to H₂O and is mainly produced in the water column by photochemical reactions involving dissolved organic matter (DOM) and O₂ [Yuan and Shiller, 2001]. Light absorbed by DOM induces an electron transfer to O₂ forming O₂⁻, which undergoes disproportionation to form H₂O₂. Typical open ocean H₂O₂ profiles show an exponential decrease from a surface maximum consistent with the downwelling irradiance. Maximum concentrations of 300 nmol L⁻¹ have been reported in Equatorial and Tropical regions with high DOM concentrations as for the Amazon plume [Croot et al., 2004]. In regions with low DOM and low sunlight, surface H₂O₂ levels are much lower with Southern Ocean values of 10–20 nmol L⁻¹ [Croot et al., 2005].

[3] Another potential source for H₂O₂ in surface seawater is from precipitation which preferentially removes H₂O₂

from the atmosphere during rain events [Cohan et al., 1999], consequently the atmospheric input at the equator and in the Inter Tropical Convergence Zone (ITCZ) is high [Croot et al., 2004; Weller and Schrems, 1993; Yuan and Shiller, 2000] compared to areas with less precipitation. H₂O₂ in the ocean is also produced biologically by phytoplankton [Palenik and Morel, 1988]. While photochemical production is considered the dominant pathway for H₂O₂ formation, in a few cases in the Southern Ocean, distinct H₂O₂ maximums at depth, corresponding to the chlorophyll maximum, suggest a significant biological source of H₂O₂ [Croot et al., 2005].

[4] Removal pathways also determine H₂O₂ concentrations in the water column and include the Catalase and Peroxidase activity of phytoplankton [Moffett and Zafiriou, 1990] along with redox reactions with reduced metals (e.g. Fe(II) and Cu(II)) [Millero and Sotolongo, 1989; Moffett and Zika, 1987]. The ‘dark decay life-time’ of H₂O₂ can vary from hours to weeks in the ocean [Petasne and Zika, 1997], but typically is around 4 days in the open ocean [Plane et al., 1987]. Overall, the decay rate of H₂O₂ is apparently controlled by several factors including H₂O₂ concentration, colloid concentration, bacteria/cyanobacteria numbers and temperature, which controls enzymatic decay [Wong et al., 2003; Yuan and Shiller, 2001]. Due to its short lifetime H₂O₂ shows potential as a tracer for recent vertical mixing activity [Johnson et al., 1989].

[5] In the present study we compare H₂O₂ profiles with physical and bio-optical measurements and available satellite data to determine the major processes controlling the distribution of H₂O₂ in the upper ocean along a meridional transect in the eastern Atlantic.

2. Methods

2.1. Sampling

[6] Samples were collected during the GEOTRACES cruise, ANTXXIII-I from 14 October to 17 November 2005 on board the German research vessel *R. V. Polarstern* on a transect between Bremerhaven and Cape Town. Six to seven depths were sampled for H₂O₂ from the upper 200 m at 19 stations (Figure 1), at local noon, using Niskin bottles on a standard CTD rosette. All analytical work was carried out in an AirClean class 100 laminar flow clean bench. Chlorophyll and chromophoric dissolved organic matter (CDOM) were measured in samples collected from the same CTD/rosette cast.

[7] By sampling only at local noon we were unable to examine the importance of the solar driven diel cycle in H₂O₂, by which variations of up to 40 nmol L⁻¹ H₂O₂ have been reported with maxima in the afternoon or early evening [Yuan and Shiller, 2001; Zika et al., 1985a; Zika

¹Alfred-Wegener-Institut für Polar- und Meeresforschung, Bremerhaven, Germany.

²FB2 Marine Biogeochemie, Leibniz-Institut für Meereswissenschaften (IFM-Geomar), Kiel, Germany.

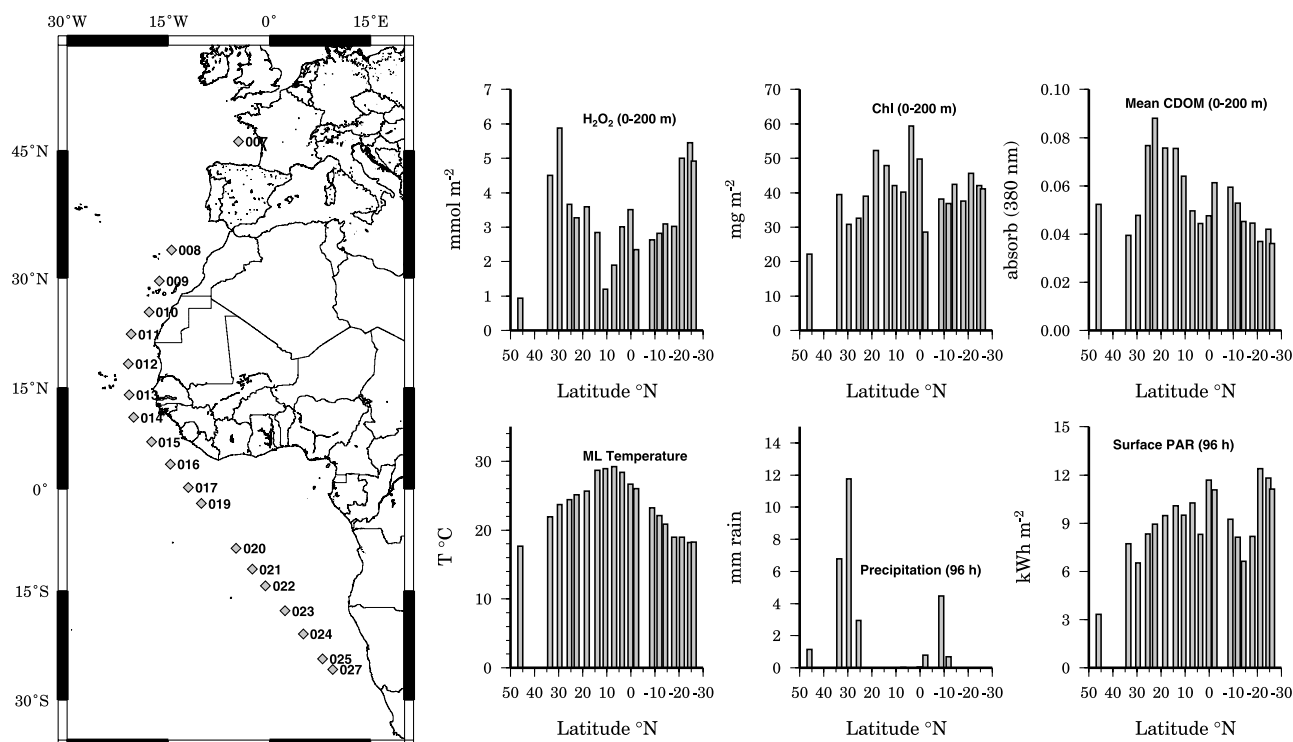


Figure 1. (left) ANTXXIII-1 cruise transect with location of the sampling stations. (right) Representative latitudinal distributions of some of the analysed parameters along the ANTXXIII-1 cruise transect. Clockwise from top left: H_2O_2 inventory (0–200 m), chlorophyll inventory (0–200 m), mean CDOM in the upper 200 m, surface PAR for the preceding 96 hours (source: HelioClim-2 database), precipitation for the preceding 96 hours (source: TRMM data), and mixed layer temperature.

et al., 1985b]. In the present work by sampling at the local noon, we are able to provide a valid comparison between stations along the transect but it is clear more work on the diel cycling of H_2O_2 is required.

2.2. H_2O_2 Measurements in Surface Waters

[8] Samples were drawn into 100 mL low density brown polyethylene bottles which were impervious to light. Unfiltered samples for H_2O_2 were analyzed within 1–2 h of collection using a flow injection chemiluminescence (FIA-CL) reagent injection method [Yuan and Shiller, 1999] as described by Croot *et al.* [2004]. Five replicates of each sample were analyzed with a typical precision of 2–3% in the concentration range of 2–120 nmol L^{-1} and a detection limit (3σ) of typically 0.6 nmol L^{-1} .

2.3. Measurement of the Natural Light Field Within the Upper Water Column

[9] A freefalling spectroradiometer (SPMR, Satlantic) was deployed for measuring the natural light field within the upper water column (down to 150–200 m). The spectral downwelling irradiance was measured at 13 wavelengths covering a spectral range from 339–682 nm.

2.4. Photosynthetically Active Radiation (PAR) Data

[10] Hourly sub-surface PAR (400–700 nm) estimates for the sampling period were obtained from the HelioClim-2 database (http://www.soda-is.com/eng/services/service_invoke/gui.php) which is constructed from METEOSAT data using the Heliosat-2 method [Rigollier *et al.*, 2004].

2.5. Measurement of Chlorophyll and CDOM Within the Upper Water Column

[11] The samples were filtered to collect the particulate matter and then stored in liquid nitrogen. Samples were analyzed post-cruise with HPLC (High Performance Liquid Chromatography) by R. A. Reynolds and D. Stramski (Scripps Institution of Oceanography, U.S.). Spectral absorption measurements of CDOM at 326 and 380 nm were made onboard the ship by R. Röttgers (GKSS Research Centre, Germany) using PSICAM [Röttgers and Doerffer, 2007].

2.6. Other Parameters

[12] Salinity, temperature and transmission were measured via a CTD (SBE 911plus, Sea-Bird Electronics). The integrated (over 3 h) precipitation data in mm were obtained from NASA TRMM (Tropical Rainfall Measuring Mission) product 3B42 using the GIOVANNI web-interface (<http://daac.gsfc.nasa.gov/techlab/giovanni/>).

2.7. Statistics

[13] A Spearman rank test was performed on the data which yielded pairwise correlation coefficients (ρ) between the parameters. All statistical analyses were done with SigmaStat 3.1 (Systat Software Inc.).

3. Results

3.1. Latitudinal Patterns of H_2O_2 , Irradiance, SST, Chlorophyll/CDOM, and Precipitation During ANT XXIII-1

[14] A transect from 46°N to 26°S across the Atlantic covers a wide range of upper ocean environments [Sarthou

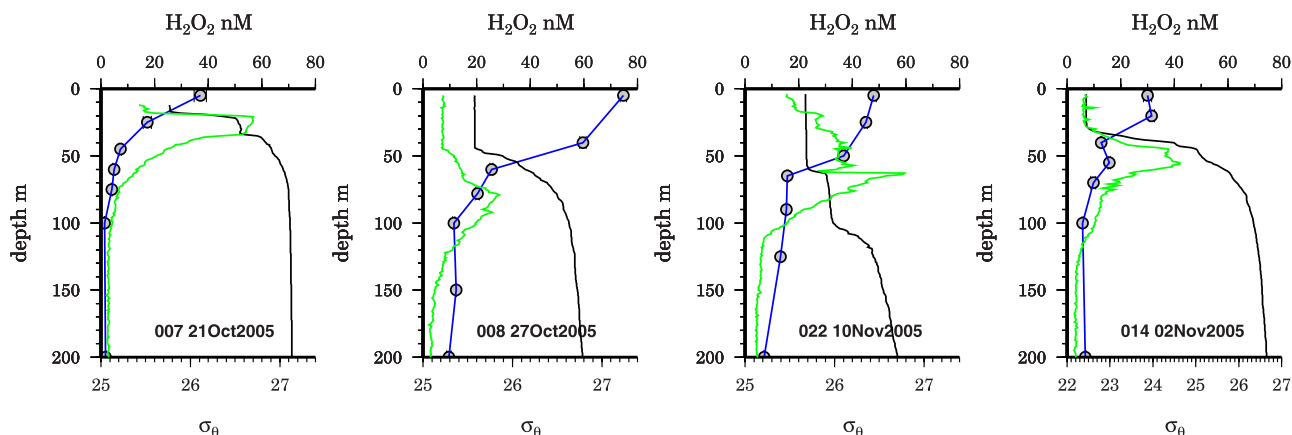


Figure 2. Vertical profiles of H₂O₂ (black circles on blue line), density σ_θ (black line), and chlorophyll fluorescence (green line, arbitrary fluorescence units where the x-axis spans from 0 to 1) showing (left) the characteristic exponential decrease (representing Stn PS 69/007, 10–13, 15–20, 24–27), (middle left) the effect of 7 mm precipitation (previous 96 h accumulated, PS 69/008), (middle right) the effect of vertical mixing (representing Stn 21–23), and (right) coinciding peaks in chlorophyll fluorescence and H₂O₂ (representing Stn 9, 14).

et al., 2003]. Surface chlorophyll concentrations ranged from 0.09–0.29 $\mu\text{g L}^{-1}$, the sea surface temperature (SST) ranged from 18–29°C with H₂O₂ inventories (0–100 m) ranging from 0.9–5.9 mmol m^{-2} (Figure 1). Highest H₂O₂ inventories between 5.5–5.9 mmol m^{-2} were found at stations 009 (30°N) and 025 (24°S), consistent with the earlier findings of *Yuan and Shiller* [2005], lowest inventories of 0.9–1.29 mmol m^{-2} at stations 007 (46°N) and 014 (10°N) (Figure 1). The highest integrated (0–200 m) chlorophyll values of 50–60 mg m^{-2} were found off Mauritania (Stn PS 69/012) and near the Equator (Stn 016) (Figure 1). CDOM absorbance, averaged over 0–200 m depth, was highest off north–west Africa (Stn 010–014) (Figure 1).

[15] Both the measured instantaneous PAR and the temperature of the mixed layer (Figure 1) reached maximum values near the Equator at station 016 and 15 respectively and decreased until station 021. Significant precipitation events (5–12 mm) occurring in the preceding 4 days before station occupation were detected for the stations off Morocco (Stn 008–009) and in the South Atlantic (Stn 021) (Figure 1).

3.2. Vertical Distribution of H₂O₂, Light, and Chlorophyll/CDOM During ANT XXIII-1

[16] The vertical profiles of H₂O₂ show the typical exponential decrease in the upper 50–100 m (Figure 2). At most of the stations H₂O₂ concentrations below 100 m depth were <10 nmol L^{-1} . Lowest surface concentrations (<30 nmol L^{-1}) were found in the Bay of Biscay (Stn PS 69/007) and at station 014 (10°N) coinciding with cloudy conditions. Maximum concentrations (123 nmol L^{-1}) were recorded in the southern Angola Basin (Stn 025) under clear skies. The vertical distribution of H₂O₂ in the Angola Basin (i.e. Stn PS 69/021–023) showed a deviation from the expected exponentially decrease, with almost constant H₂O₂ concentrations for the upper 50 m, followed by a strong decrease towards 60–80 m (Figure 2). At stations 009 and 014 small increases in H₂O₂ concentrations anom-

alous from the normal exponential pattern coincided with both the chlorophyll and CDOM maximums.

[17] Surface chlorophyll was elevated in the Bay of Biscay (Stn 007), off Mauritania (Stn 012), and in the Angola Basin (Stn 023). Vertical chlorophyll profiles showed subsurface maxima and sharp decreases with depth. Maximum surface absorbance of CDOM at 380 nm was observed in the Bay of Biscay (Stn 007) and off Mauritania (Stn 012). CDOM absorbance was low at the surface and reached highest values at the chlorophyll maximum and stayed high until 200 m depth. The average euphotic depth (1% PAR, z_{eu}) was 70 m (range 45–101 m) along the transect.

3.3. Statistical Analyses

[18] See Table 1. The vertical distribution of H₂O₂ was strongly correlated, as expected, with irradiance and was strongest at 442 nm ($\rho = 0.86$ $p < 0.05$ $\text{df} = 56$) and to a lesser extent with both PAR and UVA (340 nm). The vertical distribution of CDOM and H₂O₂ revealed a modest negative correlation ($\rho = -0.57$ $p < 0.05$ $\text{df} = 72$). H₂O₂ and chlorophyll depth distributions in turn were weakly correlated ($\rho = 0.32$ $p < 0.05$ $\text{df} = 75$). The depth of the chlorophyll maximum and the depth of maximum CDOM absorbance correlated strongly ($\rho = 0.76$ $p < 0.05$ $\text{df} = 15$, Stn 021–023 excluded due to strong mixing in the upper water column). A further strong correlation existed between vertical profiles of H₂O₂ and temperature ($\rho = 0.75$ $p < 0.05$ $\text{df} = 131$).

[19] A modest negative correlation was calculated for H₂O₂ inventories over the MLD and the average temperature over the MLD ($\rho = -0.56$ $p < 0.05$ $\text{df} = 18$), which becomes very strong ($\rho = -0.96$ $p < 0.05$ $\text{df} = 11$) excluding the stations of significant precipitation (Stn 7–10, 19–21). Strongly negative correlated were surface H₂O₂ concentrations and surface chlorophyll concentrations ($\rho = -0.75$ to -0.92). Modest and strong correlations ($\rho = 0.66$ and -0.74) were found between PAR and UVA irradiation respectively and surface H₂O₂ concentrations. Precipitation

Table 1. Results of Spearman Rank Analysis of Correlations Between H₂O₂ and Potentially Important Parameters^a

	Irradiance		Water Temperature	Chlorophyll, HPLC	CDOM, absorbance at 380 nm	Precipitation ≥ 1 mm
	PAR	340 nm				
H ₂ O ₂ Surface Data						
$\rho = \dots$	0.28(0.66)	0.40(0.74)	−0.22 (−0.44)	−0.75 (−0.92)	−0.28 (−0.11)	0.86
$p = \dots$	0.25(<0.05)	0.08(<0.05)	0.37 (0.14)	<0.05(<0.05)	0.24 (0.72)	<0.05
$df = \dots$	18(11)	18(11)	18 (11)	18 (11)	18 (11)	6
H ₂ O ₂ Inventories						
—	—	—	−0.56(−0.96) ^b < 0.05(<0.05) 18 (11)	0.20 (0.01) ^c 0.4 (0.96) 18 (11)	−0.38 (−0.40) ^d 0.11(0.19) 18 (11)	—
H ₂ O ₂ Depth profiles						
0.71 (0.72)	0.72(0.72)	0.83(0.86)	0.75 (0.65)	0.32 (0.25)	−0.57 (−0.52)	
<0.05 (<0.05)	<0.05(<0.05)	<0.05(<0.05)	<0.05 (<0.05)	<0.05 (0.09)	<0.05 (<0.05)	—
63 (40)	69 (42)	84(56)	131 (82)	75 (47)	72 (47)	

^aCorrelations measured are surface concentrations, water column inventories, and discrete concentrations at depth. Values in brackets were determined excluding stations of significant precipitation (Stn 7–10, 19–21).

^bTemperature averaged over MLD, H₂O₂ integrated over MLD.

^cIntegrated over 0–200 m.

^dCDOM absorbance averaged over 0–200 m, H₂O₂ integrated over 0–200 m.

and surface H₂O₂ values correlated strongly ($\rho = 0.86$ $p < 0.05$ $df = 6$) at the seven stations affected by rain. Excluding stations of significant rainfall generally increased the strength of the correlations in the surface data.

[20] Estimated noon sub-surface PAR values from the HelioClim-2 database were in good agreement with the measured instantaneous PAR ($\rho = 0.70$ $p < 0.05$ $df = 18$). Excluding the stations of significant precipitation (Stn 7–10 and 19–21) the sub-surface PAR estimates integrated over 24, 48 and 96 h before sampling correlated modestly with surface H₂O₂ ($\rho = 0.66$ – 0.84 $p < 0.05$ $df = 11$).

4. Discussion

[21] Our results show that the distribution and inventories of H₂O₂ observed during ANT XXIII-1 were affected by several factors related to variations in the sources, sinks and physical mixing at each location. H₂O₂ inventories were strongly negatively correlated to the SST in line with expected temperature effects on enzymatic sinks for H₂O₂ [Wong *et al.*, 2003]. Inventories of H₂O₂ decreased equatorwards in contrast to SST and daily PAR irradiance (Figure 1). The highest observed H₂O₂ inventories (0–100 m) were found at the start and near the end of the cruise (Figure 1) possibly reflecting a balance between photo-formation and temperature-dependent loss processes. The strong negative relationship between H₂O₂ and chlorophyll at the surface is probably related to increased Catalase and Peroxidase activity arising from increased phytoplankton biomass [Moffett and Zafiriou, 1990]. Latitudinal decreases in H₂O₂ suggest that sink terms are more sensitive to temperature than the photo-formation of H₂O₂ is to irradiance, a finding consistent with recent studies in the North–West Pacific [Yuan and Shiller, 2005]. Inventories of H₂O₂ decreased by 49% from station PS 69/009 to 016 despite an increase in irradiance of 49% (Figure 1), this may arise from the simultaneous increase in SST by 25% (Figure 1). However, there is a strong correlation of surface H₂O₂ and UV irradiance (340 nm) underlining the importance of UV radiation for the photo-formation of H₂O₂ [Gerringa *et al.*, 2004]. The modest to strong positive correlation of surface H₂O₂ with the preceding 24, 48 and 96 h total sub-surface PAR flux indicates that, away from areas of precipitation,

there is a clear connection to the “light history” at each station. Since instantaneous irradiation data can not solely explain distribution patterns of H₂O₂ in seawater, databases such as HelioClim-2 are a useful new tool for estimating the “light history” in the Ocean.

[22] The vertical distribution of H₂O₂ was dominated by irradiance (Table 1) with most stations showing a characteristic exponential decrease (Figure 2). The correspondence of the chlorophyll and CDOM maximum with the local increases in H₂O₂ 009 and 014 (Figure 2) suggest either; production of H₂O₂ by phytoplankton [Croot *et al.*, 2005; Palenik and Morel, 1988] or from fresh photo-labile phytoplankton exudates. Station 014 (Figure 2) shows the inverse shape of the depth profiles of CDOM and H₂O₂ causing the modest negative correlation between these parameters (Table 1) which is related to photobleaching of CDOM in surface waters [O’Sullivan *et al.*, 2005].

[23] At Station 008, high surface H₂O₂ levels show the effect of precipitation (Figures 1 and 2) on H₂O₂ levels. Although the number of rain events was small they correlated strongly with H₂O₂ surface concentrations (Table 1) confirming that rain is an important source for H₂O₂ to the surface ocean [Croot *et al.*, 2004]. In the Angola Basin (Stn 021–23), strong mixing in the upper water column with the euphotic depth (z_{eu}) and the MLD roughly equivalent, resulted in significantly higher H₂O₂ concentrations at depth than at other locations (Figure 2), highlighting the importance of upper ocean mixing processes [Johnson *et al.*, 1989] on H₂O₂ distribution. It should be noted however that strong mixing has no apparent effect on H₂O₂ inventories. The strong correlation between vertical profiles of temperature and H₂O₂ (Table 1) is not unexpected as both parameters are forced by sunlight and have similar vertical distributions, in our study region, with highest values at the surface and decreasing values with depth. Increased temperatures should shorten the lifetime of H₂O₂ [Moffett and Zika, 1987; Wong *et al.*, 2003] which is seen in the negative correlation between H₂O₂ inventories and SST.

5. Conclusion

[24] Measurements of H₂O₂ during ANT XXIII-1 show a number of factors influenced its distribution. The latitudinal

patterns observed indicate irradiance, water temperature and recent precipitation as key controls. Vertical distributions of H₂O₂ were strongly controlled by photo-formation and mixing processes in the upper water column. The recent irradiation history and phytoplankton activity appear to be the key sources and sinks in determining the observed H₂O₂ levels, with CDOM playing a minor role suggesting sunlight is the key limiting reactant in the formation of H₂O₂ in the Tropical and Sub-Tropical surface ocean. This work points to the future possibilities of developing satellite based estimations of H₂O₂ in the global ocean.

[25] **Acknowledgments.** The authors would like to show their deep thanks and appreciation to the crew of the R.V. Polarstern, for all their efforts in helping us throughout ANTXXIII-1. Thanks also to the Chief Scientist, Michiel Rutgers van der Loeff, and to the AWI for making this cruise possible. Thanks to D. Stramski, R. A. Reynolds, M. Stramska, S. Kaczmarek, R. Röttgers, K. Heymann and A. Ruser for providing the irradiance, chlorophyll and CDOM data. This manuscript was greatly improved by Uta Passow and two anonymous reviewers. The work was also partly financed by a Deutsche Forschungsgemeinschaft (DFG) project awarded to PLC (CR145/7-1) and by the DFG Excellence Cluster, "The Future Ocean". This work is also a contribution to the German SOLAS (SOPRAN) program.

References

- Cohan, D. S., M. G. Schultz, D. J. Jacob, B. G. Heikes, and D. R. Blake (1999), Convective injection and photochemical decay of peroxides in the tropical upper troposphere: Methyl iodide as a tracer of marine convection, *J. Geophys. Res.*, **104**, 5717–5724.
- Croot, P. L., P. Streu, I. Peeken, K. Lochte, and A. R. Baker (2004), Influence of the ITCZ on H₂O₂ in near surface waters in the equatorial Atlantic Ocean, *Geophys. Res. Lett.*, **31**, L23S04, doi:10.1029/2004GL020154.
- Croot, P. L., et al. (2005), Spatial and temporal distribution of Fe (II) and H₂O₂ during EISENEX, an open ocean mesoscale iron enrichment, *Mar. Chem.*, **95**, 65–88.
- Gerringa, L. J. A., et al. (2004), The influence of solar ultraviolet radiation on the photochemical production of H₂O₂ in the equatorial Atlantic Ocean, *J. Sea Res.*, **51**, 3–10.
- Johnson, K. S., et al. (1989), Hydrogen peroxide in the western Mediterranean Sea: A tracer for vertical advection, *Deep Sea Res.*, **26**, 241–254.
- Millero, F. J., and S. Sotolongo (1989), The oxidation of Fe (II) with H₂O₂ in seawater, *Geochim. Cosmochim. Acta*, **53**, 1867–1873.
- Moffett, J. W., and O. C. Zafiriou (1990), An investigation of hydrogen peroxide in surface waters of Vineyard Sound with H₂¹⁸O₂ and ¹⁸O₂, *Limnol. Oceanogr.*, **35**, 1221–1229.
- Moffett, J. W., and R. G. Zika (1987), Reaction kinetics of hydrogen peroxide with copper and iron in seawater, *Environ. Sci. Technol.*, **21**, 804–810.
- O'Sullivan, D. W., et al. (2005), Photochemical production of hydrogen peroxide and methylhydroperoxide in coastal waters, *Mar. Chem.*, **97**, 14–33.
- Palenik, B., and F. M. M. Morel (1988), Dark production of H₂O₂ in the Sargasso Sea, *Limnol. Oceanogr.*, **33**, 1606–1611.
- Petasne, R. G., and R. G. Zika (1997), Hydrogen peroxide lifetimes in south Florida coastal and offshore waters, *Mar. Chem.*, **56**, 215–225.
- Plane, J. M. C., et al. (1987), Photochemical modeling applied to natural waters, in *Photochemistry of Environmental Aquatic Systems*, edited by R. G. Zika and W. J. Cooper, pp. 215–224, Am. Chem. Soc., Washington, D. C.
- Rigollier, C., et al. (2004), The method Heliosat-2 for deriving shortwave solar radiation from satellite images, *Sol. Energy*, **77**, 159–169.
- Röttgers, R., and R. Doerffer (2007), Measurements of optical absorption by chromophoric dissolved organic matter using a point-source integrating-cavity absorption meter, *Limnol. Oceanogr. Methods*, **5**, 126–135.
- Sarthou, G., et al. (2003), Atmospheric iron deposition and sea-surface dissolved iron concentrations in the East Atlantic, *Deep Sea Res., Part I*, **50**, 1339–1352.
- Weller, R., and O. Schrems (1993), H₂O₂ in the marine troposphere and seawater of the Atlantic Ocean, *Geophys. Res. Lett.*, **20**, 125–128.
- Wong, G. T. F., et al. (2003), The decomposition of hydrogen peroxide by marine phytoplankton, *Oceanol. Acta*, **26**, 191–198.
- Yuan, J., and A. M. Shiller (1999), Determination of subnanomolar levels of hydrogen peroxide in seawater by reagent-injection chemiluminescence detection, *Anal. Chem.*, **71**, 1975–1980.
- Yuan, J. C., and A. M. Shiller (2000), The variation of hydrogen peroxide in rainwater over the South and Central Atlantic Ocean, *Atmos. Environ.*, **34**, 3973–3980.
- Yuan, J., and A. M. Shiller (2001), The distribution of hydrogen peroxide in the southern and central Atlantic ocean, *Deep Sea Res., Part II*, **48**, 2947–2970.
- Yuan, J., and A. M. Shiller (2005), Distribution of hydrogen peroxide in the northwest Pacific Ocean, *Geochem. Geophys. Geosyst.*, **6**, Q09M02, doi:10.1029/2004GC000908.
- Zika, R. G., et al. (1985a), Spatial and temporal variations of hydrogen peroxide in Gulf of Mexico waters, *Geochim. Cosmochim. Acta*, **49**, 1173–1184.
- Zika, R. G., et al. (1985b), Hydrogen peroxide concentrations in the Peru Upwelling area, *Mar. Chem.*, **17**, 265–275.

P. L. Croot, FB2 Marine Biogeochemie, Leibniz-Institut für Meereswissenschaften (IFM-Geomar), Dienstgebäude Westufer, Düsterbrookweg 20, D-24105 Kiel, Germany. (pcroot@ifm-geomar.de)

S. Steigenberger, Alfred-Wegener-Institut für Polar- und Meeresforschung, Am Handelshafen 12, D-27570 Bremerhaven, Germany.